PAPER www.rsc.org/crystengcomm | CrystEngComm

Ionic fullerene complex $(\mathrm{DMI}^+)_3\cdot(\mathrm{C}_{60}{}^{\bullet-})\cdot(\mathrm{I}^-)_2$ with 2H-hexagonal fullerene packing and 3-D DMI^+-I^- network†

Dmitry V. Konarev,*[a] Salavat S. Khasanov,[b] Akihiro Otsuka,[c] Gunzi Saito*[d] and Rimma N. Lyubovskaya[a]

Received 25th July 2008, Accepted 9th December 2008
First published as an Advance Article on the web 26th January 2009
DOI: 10.1039/b812803k

A new ionic complex of fullerene $(\mathrm{DMI}^+)_3\cdot(\mathrm{C}_{60}{}^{\bullet-})\cdot(\mathrm{I}^-)_2$ (**1**) (DMI^+ is the *N,N'*-dimethylimidazolium cation) was obtained as single crystals. The complex has a unique structure with a three-dimensional (3D) DMI^+–I^- network which arranges $\mathrm{C}_{60}{}^{\bullet-}$ radical anions. The network consists of the $(\mathrm{DMI}^+)_3\cdot(\mathrm{I}^-)$ units and is held together by the hydrogen $\mathrm{H(DMI^+)}$–(I^-) bonds. The $\mathrm{C}_{60}{}^{\bullet-}$ radical anions are located in the center of a trihedral prism from fullerenes with a center-to-center distance of 11.05 Å, providing the 2H-hexagonal 3D packing. The relatively large distances between $\mathrm{C}_{60}{}^{\bullet-}$ prevent their dimerization but allow the manifestation of a magnetic interaction between them. The Weiss temperature of −9.6 K in the 40–300 K range indicates antiferromagnetic coupling of spins. This coupling can be accompanied by the spin frustration due to the triangular arrangement of $\mathrm{C}_{60}{}^{\bullet-}$. The complex demonstrates an unusually broad EPR signal (21.5–23.1 mT) in the 82–297 K range attributed to $\mathrm{C}_{60}{}^{\bullet-}$ which has a *g*-factor value of 2.0035 at 297 K. The signal abruptly narrows below 82 K, probably due to the freezing of $\mathrm{C}_{60}{}^{\bullet-}$ rotation.

Introduction

Interest to ionic fullerene complexes is evoked by the discovery of high conductivity and magnetism in them.[1–4] For the design of such complexes, dense packing of fullerene anions in a crystal is important. The presence of short contacts between $\mathrm{C}_{60}{}^{\bullet-}$ generally results in their dimerization.[5–16] Single-bonded $(\mathrm{C}_{60}{}^-)_2$ dimers are diamagnetic since spins of $\mathrm{C}_{60}{}^{\bullet-}$ are paired to form a single C–C bond and the complex transfers from a paramagnetic to a diamagnetic state or the magnetic moment of the complex decreases.[16] For the same reason, high conductivity is also not possible in the complexes with dimerized fullerenes. Dimerization was found in metastable $\mathrm{M}\cdot\mathrm{C}_{60}$ phases (M = K, Rb, and Cs);[5,6] $\{\mathrm{Cr(C_6H_5Me)_2}\}\cdot\mathrm{C}_{60}$;[7] $\mathrm{Cp^*{}_2Cr}\cdot\mathrm{C}_{60}\cdot(\mathrm{C_6H_4Cl_2})_2$;[8,9] $\{\mathrm{Cr(C_6H_6)_2}\}\cdot\mathrm{C}_{60}\cdot\mathrm{C_6H_5CN}$;[9] $\{\mathrm{Cr(C_6H_6)_2}\}\cdot\mathrm{C}_{60}\cdot\mathrm{C_6H_4Cl_2}$;[9,10] $\mathrm{Cp_2Co}\cdot\mathrm{C}_{60}\cdot\mathrm{C_6H_4Cl_2}$;[9] $\{\mathrm{Cr(C_6H_6)_2}\}\cdot\mathrm{C}_{60}\cdot[\mathrm{Pd(dbdtc)_2}]_{0.5}$;[11] $\{\mathrm{Cr(C_6H_5\text{–}C_6H_5)_2}\}\cdot\mathrm{C}_{60}$;[12] $(\mathrm{MDABCO})_2\cdot(\mathrm{C}_{60})_2\cdot\mathrm{ET}$;[13] and fullerene complexes with positively charged gold clusters.[14] The layered $\mathrm{Me_4N}\cdot\mathrm{C}_{60}\cdot(\mathrm{THF})_{1.5}$ complex exhibits high enough conductivity (0.01 S cm^{-1} on a pressed pellet) at room temperature (RT) but the decrease of magnetic moment of the complex at 200–150 K[15] can also be evoked by dimerization.

Sterical or spatial hindrances to the close approach of fullerene anions are needed to avoid dimerization. Dimerization is absent in the $\mathrm{C}_{60}{}^{\bullet-}$ salts with $\mathrm{Ph_4P^+}$ and $\mathrm{Ph_4As^+}$ in which fullerenes are separated by bulky cations (the distances between the centers of $\mathrm{C}_{60}{}^{\bullet-}$ are about 12.5 Å).[17,18] In the complexes containing closely packed $\mathrm{C}_{60}{}^{\bullet-}$ dimerization can be suppressed if alkyl substituents of cations or solvent molecules separate the fullerene anions. For example, $\mathrm{TDAE}^{\bullet+}$ radical cations prevent dimerization in $\mathrm{TDAE}\cdot\mathrm{C}_{60}$ which contains chains of closely packed $\mathrm{C}_{60}{}^{\bullet-}$. This complex transfers to a ferromagnetic state below 16 K.[3] Polymerization of fullerenes is observed in $\mathrm{TDAE}\cdot\mathrm{C}_{60}$ only under 7 kbar pressure.[19] In two other ionic complexes $\mathrm{Cp_2Co}\cdot\mathrm{C}_{60}\cdot\mathrm{CS_2}$[20] and $\mathrm{Cp^*{}_2Ni}\cdot\mathrm{C}_{60}\cdot\mathrm{CS_2}$[21] fullerene anions are monomeric since they are separated by the $\mathrm{CS_2}$ molecules. The appearance of high conductivity and ferromagnetic or antiferromagnetic coupling of spins is expected, namely in the fullerene complexes with closely packed monomeric $\mathrm{C}_{60}{}^{\bullet-}$ radical anions. Therefore, the search for such complexes is an important condition for further development of functional compounds based on fullerenes.

In this work we obtained a novel ionic fullerene complex $(\mathrm{DMI}^+)_3\cdot(\mathrm{C}_{60}{}^{\bullet-})\cdot(\mathrm{I}^-)_2$ (**1**) (DMI^+ is the *N,N′*-dimethylimidazolium cation). Complex **1** was characterized by the spectra in the IR-, UV-visible-NIR ranges, and temperature dependent EPR and SQUID measured down to liquid helium temperatures. Complex **1** has a unique structure with a three-dimensional (3D) network formed by the DMI^+ and I^- ions, which is held together by the hydrogen $\mathrm{H(DMI^+)}$–(I^-) bonds. The network arranges $\mathrm{C}_{60}{}^{\bullet-}$ radical anions providing 2H-hexagonal 3D packing of fullerenes with relatively large distances between them. That prevents $\mathrm{C}_{60}{}^{\bullet-}$ from dimerization but allows the manifestation of antiferromagnetic coupling of spins which, due to the triangular arrangement of $\mathrm{C}_{60}{}^{\bullet-}$, can be accompanied by spin frustration. The complex demonstrates a rather broad EPR signal at room temperature and its abrupt narrowing below 82 K. The reasons for this transition are discussed.

---

[a] *Institute of Problems of Chemical Physics RAS, Chernogolovka, Moscow region, 142432, Russia. E-mail: konarev@icp.ac.ru; Fax: +007-49652-21852*

[b] *Institute of Solid State Physics RAS, Chernogolovka, Moscow region, 142432, Russia*

[c] *Research Center for Low Temperature and Materials Sciences, Kyoto University, Sakyo-ku, Kyoto, 606-8501, Japan*

[d] *Research Institute, Meijo University, 1-501 Shiogamaguchi, Tempaku-ku, Nagoya, 468-8502, Japan. E-mail: gsaito@ccmfs.meijo-u.ac.jp; Fax: +81-52-833-7200*

† Electronic supplementary information (ESI) available: IR-, UV-vis-NIR and EPR spectra of complex **1**. CCDC reference numbers 695768_and 695769. For ESI and crystallographic data in CIF or other electronic format see DOI: 10.1039/b812803k

Results and discussion

The complex was obtained by the diffusion method developed for the syntheses of ionic fullerene complexes with organic cations.[13,22,23] C_{60}, an excess of *N,N′*-dimethylimidazolium iodide (DMI·I) and reductant CH_3CH_2SNa were stirred in the *o*-dichlorobenzene/benzonitrile mixture (12 : 2). The cationic metathesis reaction occurred during the reduction to afford the DMI^+ and $C_{60}{}^{\bullet-}$ ions in solution. The −1 charged state of C_{60} was justified by the NIR spectrum of the solution. The DMI·I salt is also rather soluble in the used mixture of solvents to provide the presence of additional DMI^+ and I^- ions in the reaction mixture. The solution was filtered and the diffusion of hexane into the obtained solution for 1 month yielded the crystals of $(DMI^+)_3 \cdot (C_{60}{}^{\bullet-}) \cdot (I^-)_2$ (**1**) as high quality hexagonal prisms with a 40% yield. The composition of the complex was determined from X-ray diffraction on a single crystal. Several crystals tested from the synthesis had the same unit cell parameters. The composition of the complex was confirmed by elemental analysis.

The optical spectra of **1** (ESI†) allow the conclusion that fullerene has approximately −1 charged state in the complex. The $F_{1u}(1\text{–}3)$ C_{60} modes are observed in the spectrum of **1** at 526, 575 and 1184 cm^{-1}. The $F_{1u}(4)$ mode, which is most sensitive to the charged state of C_{60},[24] is split into three bands and positioned at 1387, 1392 and 1397 cm^{-1}. The close position of the $F_{1u}(4)$ mode was found in the spectra of other complexes containing −1 charged C_{60} (1388–1396 cm^{-1}).[4,9,24,25] The increased intensity of the band of $F_{1u}(2)$ mode at 575 cm^{-1} relative to that of $F_{1u}(1)$ mode at 526 cm^{-1} also justifies the formation of $C_{60}{}^{\bullet-}$.[24] The NIR spectrum of **1** contains two bands at 930 and 1084 nm characteristic of the $C_{60}{}^{\bullet-}$ radical anions.[9,25]

There are three DMI^+ cations per one $C_{60}{}^{\bullet-}$ and two I^- anions providing electroneutrality of the complex (Fig. 1). Fullerenes are disordered. First of all, there is the disorder between two orientations which are related by the rotation of the molecule by 60° around its threefold axis. Such disorder pattern is generally observed in the C_{60} complexes.[26] Furthermore, the threefold axis of fullerene deviates by about 4° from the threefold symmetry axis of the lattice aligned along the *c*-axis. As a result, the rotation of the fullerene molecule about the threefold axis of the lattice produces three additional orientations of C_{60}. Such disorder pattern yields totally six orientations of $C_{60}{}^{\bullet-}$. In Fig. 1 and 2a only the mean orientation of $C_{60}{}^{\bullet-}$ is depicted for clarity. One iodine anion (marked as I_A in Fig. 1) is disordered between four positions which lie in one line directed along the *c*-axis and have the 35/35/15/15% occupancies. Another ordered iodine anion (marked as I_B in Fig. 1) occupies a symmetric position in the inversion center.

An interesting feature of the complex is a three-dimensional (3D) network formed by the DMI^+ and I^- ions which arranges $C_{60}{}^{\bullet-}$ radical anions (Fig. 2). The network consists of the $(DMI^+)_3 \cdot (I_A{}^-)$ units. These units are held together by the hydrogen $H(DMI^+)\text{–}(I_A{}^-)$ bonds formed by the hydrogen atom at 2-position of the DMI^+ hetero ring and the $I_A{}^-$ anions, as shown in Fig. 2a and 2b. The $H(DMI^+)\cdots(I_A{}^-)$ distances are rather short (2.63–2.73 Å). The $(DMI^+)_3 \cdot (I_A{}^-)$ units form honeycomb layers in the *ab* plane, being connected to each other by weak hydrogen $H(DMI^+)\text{–}(I_B{}^-)$ bonds (Fig. 2a, b). The hydrogen atoms at 4- and 5-positions of the DMI^+ hetero ring are involved in this bonding. Since the $I_B{}^-$ anions are located between the $(DMI^+)_3 \cdot (I_A{}^-)$ layers they connect the neighboring $(DMI^+)_3 \cdot (I_A{}^-)$ layers into a 3D network, as shown in Fig. 2b. The $H(DMI^+)\cdots(I_B{}^-)$ distances are equal to 3.033 Å. The $I_B{}^-$ anions form continuous linear chains along the *c*-axis whereas the $I_A{}^-$ anions alternate along the *c*-axis with the $C_{60}{}^{\bullet-}$ radical anions (Fig. 2b, c). Complex **1** is a rare

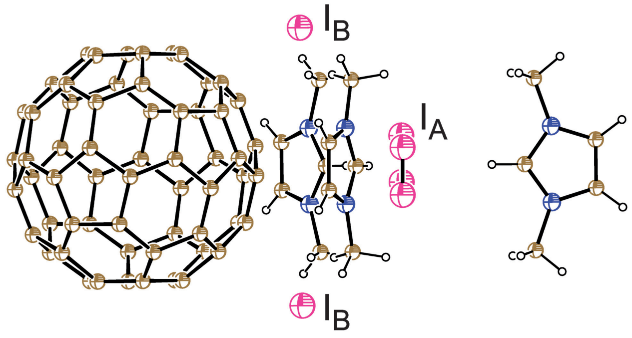

Fig. 1 Crystallographically independent units in **1**: the $C_{60}{}^{\bullet-}$ radical anion, three DMI^+ cations and two I^- anions (I_A and I_B).

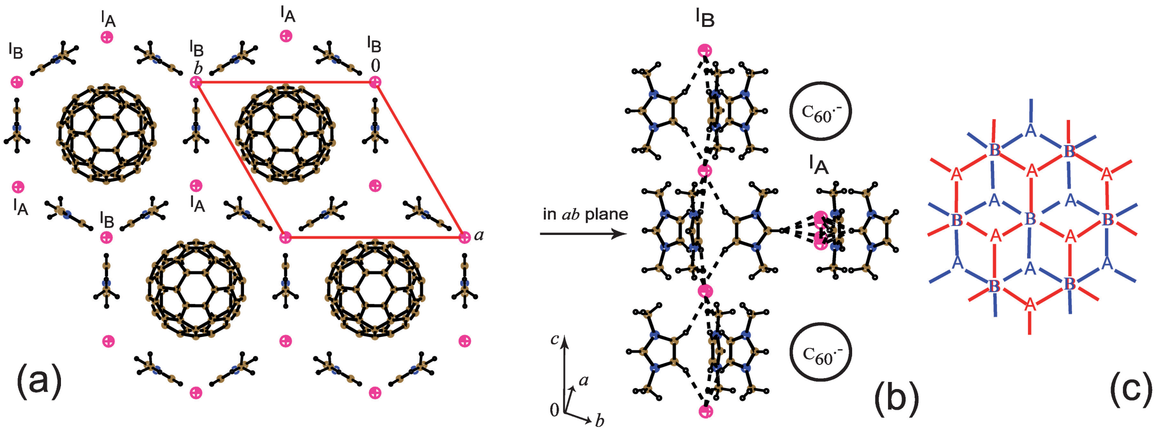

Fig. 2 (a) View of the honeycomb $DMI^+\text{–}I^-$ layer in the *ab* plane. (b) The formation of the hydrogen $H(DMI^+)\cdots(I^-)$ bonds (dashed lines) in the *ab* plane and along the *c* axis. The positions of $C_{60}{}^{\bullet-}$ are shown by circles. (c) Schematic view on the 3D $DMI^+\text{–}I^-$ network along the *c*-axis. The $I_A{}^-$ and $I_B{}^-$ anions are marked as A and B. Different $DMI^+\text{–}I^-$ layers are shown in red and blue colors.

example of a fullerene structure with a 3D ionic network formed by the hydrogen $H\cdots(I^-)$ bonds. Previously, the hydrogen $H(Ph_4P^+)$–(I^-) bonds of 2.822 Å length were found in $(Ph_4P^+)_2\cdot(C_{60}^{\bullet-})\cdot(I^-)$,[17] in which the I^- anions are surrounded by six phenyl groups of the Ph_4P^+ cations.

Each $C_{60}^{\bullet-}$ radical anion occupies honeycomb cells in the packing of the $(DMI^+)_3\cdot(I_A^-)$ units and, as a result, they form hexagonal layers in the *ab* plane (Fig. 2a). Center-to-center interfullerene distances in the layers are equal to 13.36 Å (blue dotted lines in Fig. 3). Since fullerenes are separated by the DMI^+ cations no direct van der Waals $C\cdots C$ contacts are formed between them. The hexagonal fullerene layers are shifted relative to each other in such a way that each $C_{60}^{\bullet-}$ is located below and under the center of fullerene triangles from the neighboring layers (Fig. 3). Therefore, each $C_{60}^{\bullet-}$ radical anion is located in the center of a trihedral prism formed by six fullerenes with an equal center-to-center distance of 11.05 Å (red dashed lines in Fig. 3). The distance of 11.05 Å is still not short enough to form direct van der Waals $C\cdots C$ contacts between $C_{60}^{\bullet-}$. On the whole, the arrangement of fullerenes in a crystal can be described as the 2H-hexagonal 3D packing (an analogue of hcp structure but with a loose arrangement of the units) (Fig. 3). Each $C_{60}^{\bullet-}$ is surrounded by six DMI^+ cations in the *ab* plane (Fig. 2a), and six other DMI^+ cations from neighboring layers form shortened $H(DMI^+)\cdots C(C_{60}^{\bullet-})$ contacts by methyl groups.

The magnetic properties of **1** were studied by the SQUID technique in the 1.9–300 K range. The diamagnetic temperature independent contribution and the contribution from the sample holder were subtracted from the experimental data. The effective magnetic moment of the complex is 1.64 μ_B. This value is slightly smaller than the value of 1.73 μ_B calculated for the system containing one $S = 1/2$ spin per formula unit. This spin is localized on $C_{60}^{\bullet-}$ since both DMI^+ and I^- ions are diamagnetic. The estimated Weiss temperature of −9.6 K in the 40–300 K range (Fig. 4) indicates that magnetic coupling between $C_{60}^{\bullet-}$ is predominantly an antiferromagnetic (AF) one. From structural data we can conclude that magnetic coupling in **1** can be realized between $C_{60}^{\bullet-}$ within the 2H-hexagonal 3D packing with the shortest center-to-center interfullerene distance of 11.05 Å. However, since fullerenes have a triangular arrangement in this packing the AF coupling can be accompanied by spin frustration. Previously, spin frustration was even observed in inorganic[27] and purely organic compounds[28] with a 2D triangular and Kagomé lattice as well as in the 3D molecular solids with a rutile-like structure.[29,30] Below 40 K the deviation from the Curie–Weiss law is observed showing weak ferromagnetic coupling of spins at low temperatures (Fig. 4). However, the long-range magnetic ordering is not observed down to 1.9 K.

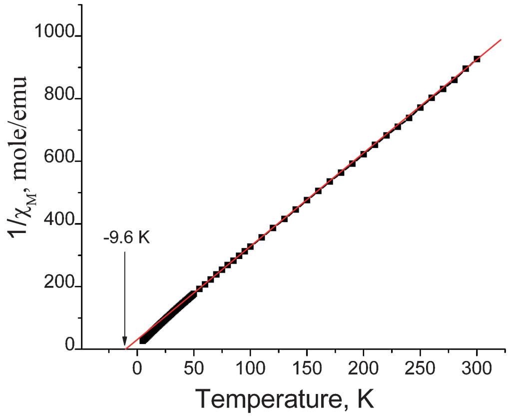

Fig. 4 Temperature dependence of reciprocal molar magnetic susceptibility fitted by the Curie–Weiss expression $\chi \propto (T - \Theta)^{-1}$ with the Θ value of −9.6 K in the 40–300 K range (red line).

The EPR spectra of **1** were studied in the 4–297 K range. The complex shows an EPR signal of the Lorenz shape with a *g*-factor of 2.0035 and the linewidth (ΔH) of 21.5 mT (297 K). Such broad EPR signal, together with a large *g*-factor value, was not previously observed in the $C_{60}^{\bullet-}$ complexes which generally manifest EPR signals with the *g*-factors in the 1.9996–2.0000 range and ΔH of 2–6 mT.[4–21,31] It should be noted that the

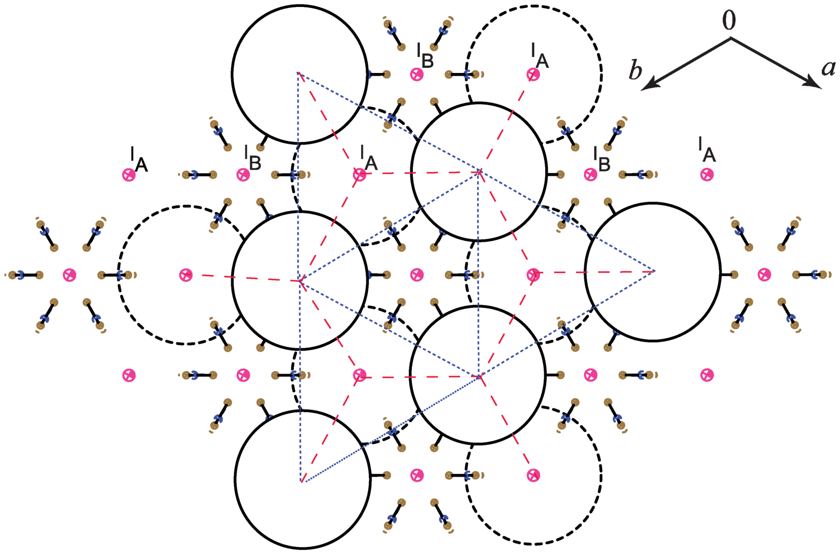

Fig. 3 View on the 2H-hexagonal fullerene packing along the *c*-axis. The $C_{60}^{\bullet-}$ radical anions are shown by circles for clarity. Center-to-center distances between $C_{60}^{\bullet-}$ of 13.36 Å are marked by blue dotted lines and those of 11.05 Å are marked by red dashed lines.

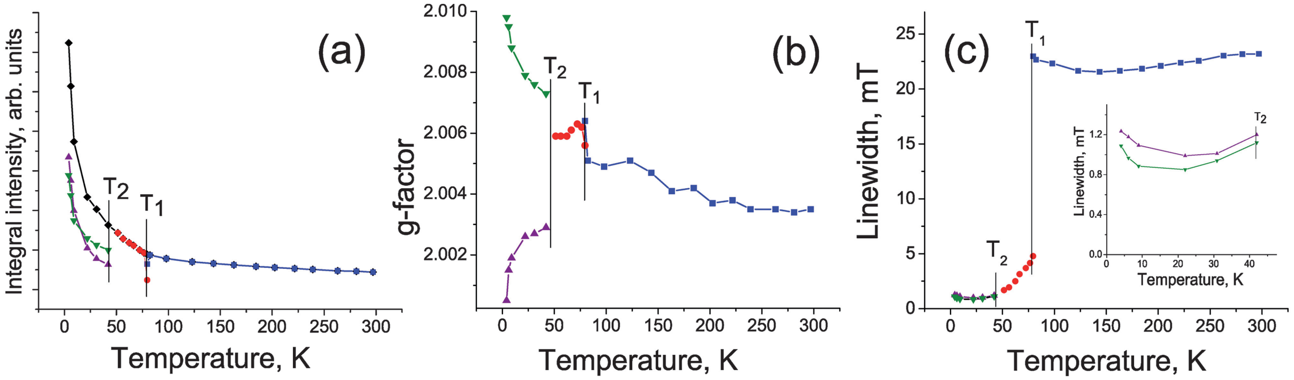

Fig. 5 Temperature dependence of the parameters of the EPR signal of **1** in the 4–297 K range: (a) the integral intensity; (b) the *g*-factor; and (c) the linewidth. T_1 indicates the temperature for narrowing of the signal below 82 K and T_2 indicates the temperature for splitting of the signal below 40 K. Insert shows the temperature dependence of the linewidth of two components of the signal below 40 K. The blue curve indicates the data for the broad signal in the 82–297 K range, the red curve indicates the data for the narrow signal in the 40–82 K range, the green and violet curves indicate the data for the two components of the split signal in the 4–40 K range.

observed signal belongs to $C_{60}^{\bullet-}$ since its integral intensity corresponds to the contribution of about one $S = 1/2$ spin per formula unit and this signal was reproduced for different samples of **1**. Temperature decrease slightly broadens the signal (ΔH of 23.1 mT at 82 K, Fig. 5c) and the *g*-factor shifts to larger values (2.0064 at 82 K, Fig. 5b). The EPR signal of **1** abruptly narrows (more than four times) below 82 K (this temperature is marked as T_1 in Fig. 5). The transition is realized within the 6 K range, and below 76 K a narrow signal of the same integral intensity is only observed. The abrupt narrowing of the EPR signal can be evoked by freezing of the $C_{60}^{\bullet-}$ rotation (which can be realized between six orientations of fullerene) and the replacement of the dynamic Jahn–Teller condition by a static one when the $C_{60}^{\bullet-}$ radical anions are trapped in one of the possible Jahn–Teller configurations. Since the overlap of electronic wave functions increases at freezing, the EPR line strongly exchange narrowed.[32,33] Previously studied $C_{60}^{\bullet-}$ complexes show gradual narrowing of the EPR signals with the temperature decrease and the linewidth of the signal being about 0.4–1 mT at 80 K.[17–21,31–35] For example, in TDAE·C_{60} the temperature of narrowing of the EPR signal coincides with the temperature of the orientational ordering of $C_{60}^{\bullet-}$. However, this transition is realized as gradual narrowing of the signal in the 150–100 K range.[32]

The line noticeably narrows in the 82–40 K range. Below 40 K the signal splits into two components which shift to the lower and higher magnetic fields with the temperature decrease and slightly broadened below 20 K (Fig. 5). Such anisotropic *g*-factors were previously found in different ionic complexes of C_{60}.[23,32–34]

Conclusion

A new ionic complex of fullerene: $(DMI^+)_3 \cdot (C_{60}^{\bullet-}) \cdot (I^-)_2$ (**1**) was obtained. This complex has an unique structure among ionic fullerene complexes since it contains a 3D network from the DMI^+ and I^- ions which is held together by the hydrogen $H(DMI^+)$–(I^-) bonds. The network accommodates $C_{60}^{\bullet-}$ radical anions. The fullerenes form a 2H-hexagonal 3D packing (an analogue of hcp structure) in which they have trihedral prismatic surrounding with the 11.05 Å interfullerene center-to-center distance. The distances between $C_{60}^{\bullet-}$ are rather large and no direct van der Waals C···C contacts are formed between them. As a result, $C_{60}^{\bullet-}$ can not dimerize down to 4 K. At the same time fullerenes are not isolated and manifest a noticeable magnetic coupling of spins which has an AF nature and can be accompanied by spin frustration. The complex manifests unusual EPR behavior. The EPR line is noticeably broader and the *g*-factor is larger than that previously observed in the complexes containing −1 charged C_{60}.[17–21,31–34] The strong narrowing of the signal below 82 K is attributed to the abrupt freezing of $C_{60}^{\bullet-}$ rotation. The complex can be a precursor for the preparation of hexagonal 3D polymers from C_{60}^- anions under pressure. The closer approach of fullerenes at the polymerization enhances the magnetic coupling between them and can increase the conductivity of the complex.

Experimental

Materials

N-Methylimidazole, sodium ethanethiolate (CH_3CH_2SNa) and methyl iodide (CH_3I) were purchased from Aldrich. C_{60} of 99.98% purity was received from MTR Ltd. The solvents were purified in argon atmosphere. *o*-Dichlorobenzene ($C_6H_4Cl_2$) was distilled over CaH_2 under reduced pressure, benzonitrile (C_6H_5CN) was distilled over Na under reduced pressure, tetrahydrofurane and hexane were distilled over Na/benzophenone. The solvents were degassed and stored in a glove box. All manipulations for the synthesis of **1** were carried out in a MBraun 150B-G glove box with controlled atmosphere with the content of H_2O and O_2 less than 1 ppm. The crystals were stored in a glove box and sealed in anaerobic conditions in 2 mm quartz tubes for SQUID and EPR measurements under 10^{-5} Torr. KBr pellets for IR- and UV-visible-NIR measurements were prepared in a glove box.

Synthesis

N,N′-Dimethylimidazolium iodide (DMI·I) was obtained by the addition of 2 molar equivalents of methyl iodide to 2 mL of *N*-methylimidazole dissolved in 20 mL of tetrahydrofurane. After 2 h, a white precipitate was filtered, which was dried under vacuum

(6 h) and was stored under helium in the glovebox. Yield is 60%. The compound was subjected to satisfactory elemental analysis.

The crystals of **1** were obtained by the following procedure. C_{60} (25 mg, 0.035 mmol), a 10-fold molar excess of CH_3CH_2SNa (30 mg, 0.36 mmol) and a 5-fold molar excess of DMI·I (39.2 mg, 0.175 mmol) were stirred in a mixture of *o*-dichlorobenzene/benzonitrile (12 : 2) for 2 h at 60 °C. During stirring, the color of the solution changed from violet to violet–brown. The NIR spectrum of the solution indicates the selective reduction of fullerene to the −1 charged state. The mixture was cooled, filtered in a 50 mL glass tube of 1.8 cm diameter with a ground glass plug, and 30 mL of hexane was layered over the solution. The diffusion was carried out during 1 month to give the crystals of **1** on the wall of the tube. The solvent was decanted from the crystals, which were washed with hexane to give black prisms up to $1 \times 1 \times 0.5$ mm^3 in size with a 40% yield. The composition of the complex was determined by the X-ray diffraction on a single crystal: $(DMI)_3 \cdot C_{60} \cdot I_2$ (**1**). Several single crystals selected from the synthesis have the same unit cell parameters. Elemental analysis of **1**: $C_{75}H_{27}N_6I_2$; Found C 70.02, H 2.06; N 6.32; I 20.44%; Calc., C 71.15, H 2.13, N 6.64, I 20.07%.

General

UV-visible-NIR spectra were measured in KBr pellets on a Shimadzu-3100 spectrometer in the 240–2600 nm range. FT-IR spectra were measured in KBr pellets with a Perkin-Elmer 1000 Series spectrometer (400–7800 cm^{-1}). EPR spectra were recorded for a polycrystalline sample from 4 up to 300 K with a JEOL JES-TE 200 X-band ESR spectrometer equipped with a JEOL ES-CT470 cryostat. The *g*-factor was calibrated against α,α'-diphenyl-β-pycrylhydrazyl (DPPH). A Quantum Design MPMS-XL SQUID magnetometer was used to measure the static magnetic susceptibility of polycrystalline **1** between 300 and 1.9 K at 100 mT static magnetic field. A sample holder contribution and core temperature independent diamagnetic susceptibility (χ_0) were subtracted from the experimental data. The values of C, Θ and χ_0 were calculated in a high-temperature range using the appropriate formula: $\chi_M = C/(T - \Theta) + \chi_0$ and the experimental data in the 40–300 K range. The effective magnetic moment of **1** was calculated using the formula: $\mu_{eff} = (8\chi_M T)^{1/2}$.

X-Ray crystal structure determination

Crystal data of 1. $C_{75}H_{27}I_2N_6$, M_r = 1265.83 g mol^{-1}, black prisms, trigonal, $P\bar{3}1c$, $a = b = 13.3617(2)$, $c = 15.8651(5)$ Å, $\alpha = \beta = 90°$, $\gamma = 120°$, $V = 2453.00(9)$ Å^3, $Z = 2$, $d_{calc} = 1.714$ g cm^{-3}, $\mu = 1.342$ mm^{-1}, $F(000) = 1250$, $T = 100$ (2) K, $2\theta_{max} = 65.56°$, reflections measured 22635, unique reflections 3005, reflections with $I > 2\sigma(I) = 2566$, parameters refined 406, restrains 7851, $R_1 = 0.0772$, $wR_2 = 0.2401$, G.O.F. = 1.081.

The intensity data for the structural analysis were collected using a Bruker Nonius X8 Apex diffractometer with a CCD area detector (Mo Kα radiation, λ = 0.71073Å) equipped with an Oxford Cryosystems nitrogen gas-flow apparatus. The data were collected by φ- and ω-scans with 0.3° frame-width and 30 s exposure time per frame. The data were integrated, scaled, sorted and averaged using the Bruker AXS software package.[36] The structure was solved by a direct method and refined by the full-matrix least-squares method against F^2 using SHELX-97.[37]

Non-hydrogen atoms were refined in the anisotropic approximation. The positions of the hydrogen atoms were calculated geometrically. Subsequently, the positions of the H atoms were refined by the "riding" model with $U_{iso} = 1.2U_{eq}$ of the connected non-hydrogen atom or as ideal CH_3 groups with $U_{iso} = 1.5U_{eq}$. To keep the fullerene geometry close to the ideal one in the severely disordered group the bond length restraints were applied along with the next-neighbor distances, using the SADI *SHELXL* instruction. To keep the anisotropic thermal parameters of the fullerene atoms within reasonable limits the displacement components were restrained using ISOR and DELU *SHELXL* instructions.

List of abbreviations

$Cr(C_6H_5Me)_2$	Bis(toluene)chromium
$Cp^*{}_2Cr$	Decamethylchromocene
$Cr(C_6H_6)_2$	Bis(benzene)chromium
Cp_2Co	Cobaltocene
$Pd(dbdtc)_2$	Palladium (II) dibenzyldithiocarbamate
$Cr(C_6H_5–C_6H_5)_2$	Bis(diphenyl)chromium
ET	Bis(ethylenedithio)tetrathiafulvalene
$MDABCO^+$	*N*-Methyldiazabicyclooctane cation
$Cp^*{}_2Ni$	Decamethylnickelocene
Ph_4P^+	Tetraphenylphosphoniun cation
Ph_4As^+	Tetraphenylarsonium cation
DMI^+	*N,N'*-Dimethylimidazolium cation

Acknowledgements

The work was supported by RFBR grant N 06-03-32824 and Grant-in-Aid Scientific Research from the Ministry of Education, Culture, Sports, Science and Technology, Japan (152005019, 21st Century COE).

References

1 M. J. Rosseinsky, *J. Mater. Chem.*, 1995, **5**, 1497.
2 H. Kobayashi, H. Tomita, H. Moriyama, A. Kobayashi and T. Watanabe, *J. Am. Chem. Soc.*, 1994, **116**, 3153.
3 P.-M. Allemand, K. C. Khemani, A. Koch, F. Wudl, K. Holczer, S. Donovan, G. Grüner and J. D. Thompson, *Science*, 1991, **253**, 301.
4 D. V. Konarev and R. N. Lyubovskaya, *Russ. Chem. Rev.*, 1999, **68**, 19.
5 Q. Zhu, D. E. Cox and J. E. Fischer, *Phys. Rev. B*, 1995, **51**, 3966.
6 G. Oszlányi, G. Bortel, G. Faigel, M. Tegze, L. Grárásy, S. Pekker, P. W. Stephens, G. Bendele, R. Dinnebier, G. Mihály, A. Jánossy, O. Chauvet and L. Forró, *Phys. Rev. B*, 1995, **51**, 12228.
7 A. Hönnerscheid, L. Wüllen, M. Jansen, J. Rahmer and M. Mehring, *J. Chem. Phys.*, 2001, **115**, 7161.
8 D. V. Konarev, S. S. Khasanov, A. Otsuka and G. Saito, *J. Am. Chem. Soc.*, 2002, **124**, 8520.
9 D. V. Konarev, S. S. Khasanov, G. Saito, A. Otsuka, Y. Yoshida and R. N. Lyubovskaya, *J. Am. Chem. Soc.*, 2003, **125**, 10074.
10 D. V. Konarev, S. S. Khasanov, A. Y. Kovalevsky, G. Saito, A. Otsuka and R. N. Lyubovskaya, *Dalton Trans.*, 2006, 3716.
11 D. V. Konarev, A. Y. Kovalevsky, A. Otsuka, G. Saito and R. N. Lyubovskaya, *Inorg. Chem.*, 2005, **44**, 9547.
12 G. A. Domrachev, Y. A. Shevelev, V. K. Cherkasov, G. V. Markin, G. K. Fukin, S. Y. Khorshev, B. S. Kaverin and V. L. Karnatchevich, *Russ. Chem. Bull.*, 2004, **53**, 2056.
13 D. V. Konarev, S. S. Khasanov, G. Saito, A. Otsuka and R. N. Lyubovskaya, *J. Mater. Chem.*, 2007, **17**, 4171.

14 M. Schulz-Dobrick and M. Jansen, *Angew. Chem., Int. Ed.*, 2008, **47**, 2266.
15 R. E. Douthwaite, M. A. Green, M. L. H. Green and M. J. Rosseinsky, *J. Mater. Chem.*, 1996, **6**, 1913.
16 D. V. Konarev, S. S. Khasanov and R. N. Lyubovskaya, *Russ. Chem. Bull.*, 2007, **56**, 371.
17 A. Pènicaud, A. Peréz-Benítez, V. R. Gleason, P. E. Muñoz and R. Escudero, *J. Am. Chem. Soc.*, 1993, **115**, 10392.
18 U. Bilow and M. Jansen, *Z. Anorg. Allg. Chem.*, 1995, **621**, 982.
19 S. Garaj, T. Kambe, L. Forró, A. Sienkiewicz, M. Fujiwara and K. Oshima, *Phys. Rev. B*, 2003, **68**, 144430.
20 A. L. Balch, J. W. Lee, B. C. Noll and M. M. Olmstead, *Proc. Electrochem. Soc.*, 1994, **94–24**, 1231.
21 W. C. Wan, X. Liu, G. M. Sweeney and W. E. Broderick, *J. Am. Chem. Soc.*, 1995, **117**, 9580.
22 D. V. Konarev, S. S. Khasanov, A. Otsuka, G. Saito and R. N. Lyubovskaya, *Chem.–Eur. J.*, 2006, **12**, 5225.
23 D. V. Konarev, S. S. Khasanov, A. Otsuka, G. Saito and R. N. Lyubovskaya, *Inorg. Chem.*, 2007, **46**, 2261.
24 T. Picher, R. Winkler and H. Kuzmany, *Phys. Rev. B*, 1994, **49**, 15879.
25 N. V. Semkin, N. G. Spitsina, S. Krol and A. Graja, *Chem. Phys. Lett.*, 1996, **256**, 616.
26 D. V. Konarev, I. S. Neretin, Y. L. Slovokhotov, E. I. Yudanova, N. V. Drichko, Yu. M. Shul'ga, B. P. Tarasov, L. L. Gumanov, A. S. Batsanov, J. A. K. Howard and R. N. Lyubovskaya, *Chem.–Eur. J.*, 2001, **7**, 2605.
27 S. J. Clarke, A. J. Fowkes, A. Harrison, R. M. Ibberson and M. J. Rosseinsky, *Chem. Mater.*, 1998, **10**, 372.
28 K. Awaga, T. Okuno, A. Yamaguchi, M. Hasegawa, T. Inabe, Y. Maruyama and N. Wada, *Phys. Rev. B*, 1994, **49**, 3975.
29 J. L. Manson, C. Campana and J. S. Miller, *Chem. Commun.*, 1998, 251.
30 J. L. Manson, E. Ressouche and J. S. Miller, *Inorg. Chem.*, 2000, **39**, 1135.
31 D. V. Konarev, A. Y. Kovalevsky, S. S. Khasanov, G. Saito, A. Otsuka and R. N. Lyubovskaya, *Eur. J. Inorg. Chem.*, 2005, 4822.
32 R. Blinc, K. Pokhodnia, P. Cevc, D. Arčon, A. Omerzu, D. Mihailovic, P. Vertirini, L. Golič, Z. Trontelj, J. Lužnik, Z. Jegličič and J. Pirnat, *Phys. Rev. Lett.*, 1996, **76**, 523.
33 G. Völkel, A. Pöppl, J. Simon, J. Hoentsch, S. Orlinskii, H. Klos and B. Gotschy, *Phys. Rev. B*, 1995, **52**, 10188.
34 J. Stinchcombe, A. Pénicaud, P. Bhyrappa, P. D. W. Boyd and C. A. Reed, *J. Am. Chem. Soc.*, 1993, **115**, 5212.
35 C. A. Reed and R. D. Bolskar, *Chem. Rev.*, 2000, **100**, 1075.
36 *Bruker Analytical X-ray Systems*, Madison, WI, USA, 1999.
37 G. M. Sheldrick, *SHELX97*, The University of Göttingen, Germany, 1997.